ORIGINAL ARTICLE

A novel single nucleotide mutation of *TFL1* alters the plant architecture of *Gossypium arboreum* through changing the pre-mRNA splicing

Ji Liu[1,2] · Pengfei Miao[1,2] · Wenqiang Qin[1,2] · Wei Hu[2] · Zhenzhen Wei[2] · Wusi Ding[1,2] · Huan Zhang[1,2] · Zhi Wang[1,2,3]

Abstract

Key message **A single nucleotide mutation from G to A at the 201st position changed the 5′ splice site and deleted 31 amino acids in the first exon of *GaTFL1*.**

Abstract Growth habit is an important agronomic trait that plays a decisive role in the plant architecture and crop yield. Cotton (*Gossypium*) tends to indeterminate growth, which is unsuitable for the once-over mechanical harvest system. Here, we identified a determinate growth mutant (*dt1*) in *Gossypium arboreum* by EMS mutagenesis, in which the main axis was terminated with the shoot apical meristem (SAM) converted into flowers. The map-based cloning of the *dt1* locus showed a single nucleotide mutation from G to A at the 201st positions in *TERMINAL FLOWER 1* (*GaTFL1*), which changed the alternative RNA 5′ splice site and resulted in 31 amino acids deletion and loss of function of *GaTFL1*. Comparative transcriptomic RNA-Seq analysis identified many transporters responsible for the phytohormones, auxin, sugar, and flavonoids, which may function downstream of *GaTFL1* to involve the plant architecture regulation. These findings indicate a novel alternative splicing mechanism involved in the post-transcriptional modification and *TFL1* may function upstream of the auxin and sugar pathways through mediating their transport to determine the SAM fate and coordinate the vegetative and reproductive development from the SAM of the plant, which provides clues for the *TFL1* mechanism in plant development regulation and provide research strategies for plant architecture improvement.

Keywords *Gossypium arboreum* · Determinate growth · *TFL1* · Plant architecture

Introduction

Flowering plants naturally display two types of plant architecture: indeterminate and determinate growth. Considering the indeterminate plants, the main axis can grow unlimitedly and produce flowers on its flank tissues. For determinate plants, the main stem growth is limited and terminated when the shoot apical meristem (SAM) turns into a flower or other reproductive structure and stops continuing to elongate indefinitely (Bradley et al. 1997; Eberwein et al. 2009; Wu et al. 2011).

Determinate growth contributes to a significant and favorable effect on the genetic improvement of many crops such as rapeseed, tomato, cotton, and so on (Jia et al. 2019; Pnueli et al. 1998; Si et al. 2018). The wild type of *Gossypium* spp. has an indeterminate inflorescence and plant architecture. With the realization of cotton production mechanization, the determinate architecture of plants is favorable for cotton mechanical harvest and production, and improving the indeterminate growth habits is a crucial project that breeders and plant scientists encounter. So, revealing the molecular mechanisms underlying the transformation between indeterminate and determinate inflorescence/architecture traits is very important to crop breeding.

Ji Liu and Pengfei Miao have contributed equally to this work.

✉ Zhi Wang
wangzhi01@caas.cn

1 National Nanfan Research Institute (Sanya), Chinese Academy of Agricultural Sciences, Sanya 572024, China

2 National Key Laboratory of Cotton Bio-breeding and Integrated Utilization, Institute of Cotton Research, Chinese Academy of Agricultural Sciences, Anyang 455000, China

3 Hainan Yazhou Bay Seed Laboratory, Sanya 572025, China

The vegetative-reproductive switch is a delicate process mediated by various genetic pathways including photoperiod, gibberellins, nitric oxide, and autonomous pathways (Amasino and Michaels 2010; Boss et al. 2004; Jack 2004). Some key regulators responsible for the floral identity and the fate of SAMs have been identified and studied well. Some homologous phosphatidyl ethanolamine-binding proteins (PEBPs)—TERMINAL FLOWER1 (TFL1)/CENTRORADIALIS (CEN)/SELF-PRUNING (SP) in *Arabidopsis*, *Antirrhinum*, *Cucumber*, tomato as well as *Gossypium barbadense* have been evidenced to play a key role in the maintenance of SAM indeterminate status and floral identity establishment (Bradley et al. 1996, 1997; Shannon and Meeks-Wagner 1991; Wen et al. 2019). It is found that TFL1 and another PEBP-FLOWERING LOCUS T (FT) function antagonistically to regulate the floral transition as mobile RNA or protein in *Arabidopsis*. In the reciprocal pathway, TFL1 represses and FT activates the flowering transition, respectively, consequently playing crucial roles in the inflorescence pattern and plant architecture (Baumann et al. 2015; Shannon and Meeks-Wagner 1991; Wickland and Hanzawa 2015).

In cotton, the homologous of TFL1 and FT have been identified the key roles in plant architecture in *G. hirsutum* and *G. barbadense* (Chen et al. 2018; McGarry et al. 2016; Si et al. 2018). However, the narrow genetic base from repeated selective breeding in allotetraploid cotton restricts the development of novel and high-quality varieties. *Gossypium arboreum* presents some inherent characteristics that the allotetraploid cotton lack, such as the tolerance to drought and salinity and remarkable resistance to pests (e.g., bollworms and leafhoppers) (Nibouche et al. 2008; Tahir et al. 2011) and disease (e.g., rust, fungal and viral) (Akhtar et al. 2010; Wheeler et al. 1999). Moreover, natural *G. arboreum* (also known as Asiatic cotton, a diploid species) exhibits various colorful fibers (e.g., white, green, and tan) and some of the varieties produce high-strength fibers (Mehetre et al. 2003), which provide potential in new cultivar breeding facilitate to the gene pool diversity (Sethi et al. 2015). However, until now, determinate plants or responsible genes has not been reported in *G. arboreum*. Here, we mutated the *G. arboreum* cultivar Shixiya 1 with EMS and screened a determinate mutant—*determinate-growth 1*. The gene cloning with BSA and QTL approaches identified the *DETERMINATE-GROWTH 1*, a novel mutant allele of *TFL1* homolog, reconfirming the key role of *TFL1* in the plant architecture of *Gossypium* spp. including allotetraploid as well as diploid cotton. More interestingly, the identified novel mutation site provides clues for a kind of alternative splicing mechanism illumination in the plant.

Materials and methods

Plant materials and growth condition

Gossypium arboreum acc. Shixiya 1, an indeterminate growth plant, with indeterminate inflorescence and branches, was obtained from South China, Yangtze and Yellow River regions, which was used as a background material to obtained determinate growth mutant *dt1* by EMS mutagenesis. *G. arboreum* acc. MZM971, an indeterminate growth plant, originated in America, which was used as paternal material to construct a F_2 population. In this study, in view of the fact that Shixiya 1 and MZM971 are unsuitable for gene function verification via the virus-induced gene silencing (VIGS) technology system, *G. arboreum* acc. DQJ, another indeterminate growth plant, planted in Zhao County, Hebei Province, China, was used for the VIGS assay. All the plants were sown in the experimental field of the Institute of Cotton Research, Chinese Academic Agricultural Sciences (ICR, CAAS, Anyang, Henan Province, or Sanya, Hainan Province).

Identification of the *determinate-growth 1* in EMS-induced mutation population of *G. arboreum*

In order to obtain abundant mutants with novel traits, approximate 15,000 seeds of Shixiya 1 were presoaked in phosphate buffer (100 mM, pH 7.0) for 12 h at 28 ℃. Then, the seeds were soaked in EMS (0.6%, ethyl methane sulfonate) phosphate buffer for 8 h in the dark at 28 ℃ with continuous flip and shake during the period. Subsequently, the seeds were rinsed with distilled water for 30 min with three times to remove residual EMS. Finally, they were sown in the experimental field of ICR, CAAS (Sanya). The M_2 seeds were harvested by collecting one boll per plant from the surviving 7987 M_1 plants (53.3% survival). After four generations of self-fertilization, 123 individual lines with visible phenotypes were identified out of 5980 M_7 plants, and one of which exhibited determinate growth and was named as *determinate-growth 1* (*dt1*).

F$_2$ population construction and super bulked segregant analysis (BSA) sequencing

To clone the causal locus, the *dt1* and MZM 971 were crossed to construct a hybrid line (100 F_1 lines) in 2016, and an F_2 population (1000 plants) was generated by self-fertilization of the F_1 population in 2017. Fresh young leaves

were collected from parental lines (MZM 971 and *dt1*), 30 F_2 individual plants exhibiting indeterminate growth and 30 F_2 individual plants exhibiting determinate growth. Genomic DNA was extracted from the leaves following the previously reported method (Gong et al. 2018; Li et al. 2019). Two DNA pools were constructed. One pool consisted of DNAs from 30 F_2 plants showing the dominant phenotype (indeterminate growth), and another pool consisted of DNAs from 30 F_2 plants showing recessive phenotype (determinate growth). The experimental process is performed according to the standard protocol provided by Illumina for BSA-sequencing. The DNA of each sample was randomly broken into 350 bp fragments by ultrasonic fragmentation to construct the sequencing library. The library was sequenced by Illumina HiSeq after passing the quality inspection. Each sample was sequenced at 30×coverage of the assembled genome with 150-bp paired-end reads. Clean reads were mapped to the *Gossypium arboreum* (A2) 'SXY1' genome CRI-updated_v1 (https://www.cottongen.org/species/Gossypium_arboreum/CRI-A2_genome_v1.0) by BWA after filtering the raw reads. According to the positioning results of clean reads in the reference genome, Picard was used for mark duplicates, GATK for local realignment, base recalibration and other preprocessing to ensure the accuracy of the detected single nucleotide polymorphisms (SNPs). The SNP was further detected by GATK and filtered to obtain the final SNP site set. The average ΔSNP index was calculated based a 1000 kb sliding window with a 10 kb step size to identify regions associated with target trait.

Development and utilization of KASP marker in the *GaDT1* cloning

According to the distribution and density of SNP physical locations, KASP (Kompetitive Allele Specific PCR) markers design was performed on candidate SNPs using the online platform PolyMarker website (http://www.polymarker.info/) of HuaZhi Biotechnology Co., LTD, and chromosome-specific markers were selected from them. The FAM or HEX fluorescent linker sequence was added to the 5′ end of the KASP markers forward primer, and the FAM linker sequence was 5′-GAAGGTGACCAAGTTCATGCT-3′, the HEX linker sequence was 5′-GAAGGTCGGAGT CAACGGATT-3′. Then, the KASP markers were used for haplotype analysis in the population. If different genotypes of SNPs could be distinguished, the marker was specific and could be used for molecular assisted selection. Based on the BSA result, we found a significant single signal on Chr07 indicating that the determinate growth trait was controlled by a single locus, and designed KASP markers within the candidate region (Chr07: 5.74 Mb to 25.55 Mb). The sequence of primer GH900009 marked on the left side

of the positioning interval was: GH900009F_FAM: GAA GGTGACCAAGTTCATGCTGATCATGTTCGTTGC CTTCGTAATG; GH900009F_HEX: GAAGGTCGGAGT CAACGGATTGATCATGTTCGTTGCCTT-CGTAATC; GH900009R: AGGAAGGAGAGATGGACGCTGACAT. The sequence of the primer GH900028 marked on the right was: GH900028F_FAM: GAAGGTGACCAAGTTCAT GCTGCAACTAAACGCACCACCCATTAC; GH900028F_ HEX: GAAGGTCGGAGTCAACGGATTGCAACTAAA CGCACCAC-CCATTAT; GH900028R: TAATATTTCCCT CCCTAGCCCCTCCT.

RNA-seq and RT-qPCR analysis

Due to the formation of the terminal flower in the *dt1* mutant, the terminal buds in the different stages T1 (seedling stage, three true leaves), T2 (the early stage of flower bud formation, no visible flower buds) and T3 (flower budding stage, with visible flower buds) were taken from the wild type Shixiya 1 and the mutation line *dt1*, respectively. Total RNA was extracted by NEBNext® Ultra™ Directional RNA Library Prep Kit for Illumina® and used for RNA sequencing. Then two libraries (150 bp-length pair-end reads) were constructed in the same manner and sequenced on Illumina NovaSeq 6000 platform (Novogene, Beijing) following the protocol provided by the company (Illumina, San Diego). Clean reads were aligned to the *G. arboreum* reference genome through the Bowtie software (Li et al. 2009; Langmead and Salzberg 2012). Differentially expressed genes (DEGs) were analyzed by Cufflinks software for FPKM (fragments per kilo bases per million reads) calculation (Trapnell et al. 2010). Benjamini and Hochberg's approach was used to adjust the *P*-value for the false discovery rate. Genes with an adjusted *P*-value < 0.05 and absolute fold change value > 2 were designated as DEGs. The KAAS (https://www.genome.jp/tools/kaas/) was used for pathway annotation analysis of the DEGs. The RT-qPCR assays were performed by the 2 × Wiz Universal SYBR Green qPCR Master Mix (BCS, No. SPE00005). The *GaHis3* (Cotton_A_11188) was used as the endogenous reference gene for relative quantitation of the gene expression data (Gong et al. 2017). The relative expression levels were calculated using the $2^{-\Delta\Delta Ct}$ method (Livak and Schmittgen 2001). The sequences of each pair of primers used for the different RT-qPCR assays were listed in the Table S1.

Virus-induced gene silencing (VIGS) assay

For the VIGS assay, we used the TRV vector (i.e., pTRV1 and pTRV2), along with VIGS positive control pTRV2–*PDS*, and negative control (NC) empty vector pTRV2. A 302 bp

GaTFL1 fragment was cloned from the SAM of Shixiya 1 cDNA with the pTRV2-*GaTFL1* F/pTRV2-*GaTFL1* R primer pair (Table S1). The pTRV1 helper plasmid, pTRV2, pTRV2-*PDS*, pTRV2-*GaTFL1* were all introduced into the *Agrobacterium* strain GV3101. VIGS assay and silencing efficiency check were performed with *G. arboretum* DQJ as donor plant according to the previously published protocol (Gong et al. 2017).

Microscopy observation of SAM in WT and *dt1*

To analyze the SAM of WT and *dt1*, the terminal buds in the different stages S_1 (1 true leaf), S_2 (2 true leaves), S_3 (3 true leaves), S_4 (4 true leaves) and S_5 (5 true leaves) were taken from the wild type Shixiya 1 and the mutant line *dt1*, respectively. The samples were fixed in 4% (w/v) paraformaldehyde, 0.25% (w/v) glutaraldehyde and 50 mM sodium phosphate (pH 7.2), dehydrated by passage first through an ethanol series and then through a *t*-butanol series, embedded in paraffin, and finally sectioned to 8 μm by a Leica RM2235 rotary microtome. The paraffin sections were stained with toluidine blue and observed under the Olympus BX53 microscope.

Results

The identification of the *determinate-growth 1* mutant

To study the plant architecture regulation in *G. arboreum*, the EMS mutation was made with the Shixiya 1 and a homozygous *determinate-growth 1* (*dt1*) plant was identified from the mutant population in M_1–M_7 plants. Compared with the wild type Shixiya 1, the SAM of the *dt1* mutant differentiated into a flower bud and then formed a terminal flower, and terminated indeterminate growth, causing an approximate half decrease in plant height (Fig. 1a–c). Meanwhile, axillary buds also developed directly into flowers, showing determinate growth phenotype (Fig. 1d, e). Therefore, we sliced the terminal buds of *dt1* mutant and WT to analyze the cytological difference during different development stages. The results showed that there was no significant difference in the terminal bud differentiation between the wild type Shixiya 1 and the *dt1* mutant at the stage of one-true leaf (S1) and two-true leaves (S2). However, at the three-true-leaf stage (S3), the terminal buds of the wild type Shixiya 1 continued to differentiate to new leaves and vegetative organs, remaining indeterminate growth, the differentiation ability of the terminal buds of the *dt1* mutant was significantly changed and formed the flower meristems

and sepals gradually. In the following stages (S4 and S5), the clear leaf and stem primordium formed in the WT, while only a mature flower primordium formed in *dt1* (Fig. 2), which explained the reason for the formation of the terminal flower at the main stem in *dt1*.

The *DT1* locus is located on a 0.85 Mb genomic region on chromosome A07 by BSA analysis and fine mapping

To identify the causal locus for determinate growth of *dt1*, a *G. arboreum* line MZM 971 (indeterminate growth) and the *dt1* (determinate growth) were used as parents to construct a F_2 population through hybridization and selfing. All F_1 plants exhibited indeterminate growth, indicating that the determinate growth allele is recessive. The F_2 population produced a 3:1 segregation ratio of indeterminate growth to determinate growth phenotypes (Table S2), indicating that a single locus controlled the determinate growth of *dt1*. Then, the bulked segregation analysis (BSA) was applied to identify the causal locus and the results showed that the ΔSNP index greater than 99% confidence intervals located on chromosome A07 from 7.31 Mb to 24.57 Mb (Fig. 3a) by aligning the sequence reads to the reference Shixiya 1 genome, demonstrating that the locus controlling the determinate growth is located on chromosome A07. Based on the above candidate interval, we first developed 22 KASP markers covering the genomic region from 5,744,881 bp (SNP marker GH900009) to 25,545,712 bp (SNP marker GH900028) (Table S1). Using these markers, we performed genotype testing in 150 recessive lines in the F_2 generation population, and found that the determinate growth trait was closely linked to the 18.49–19.34 Mb interval, located at the 0.85 Mb genomic region between KASP markers SNP-GH900036 (pos.18496770) and SNP-GH900037 (pos.19341956) (Fig. 3b).

Cloning of the *GaDT1*

There are 28 genes in the region from 18,496,770 to 19,341,956 on chromosome A07 of *G. arboreum* (Table S3) (*Cotton Functional Genomics Database:* https://cottonfgd.org/). *We aligned the nucleic acids after sequencing of the 28 candidate genes between the two parents and found that Ga07G1189 had an SNP in the first exon, Ga07G1199 and Ga07G1205 possessed SNPs in introns and 9 genes (Ga07G1192, Ga07G1195, Ga07G1197, Ga07G1200, Ga07G1202, Ga07G1204, Ga07G1206, Ga07G1207, Ga07G1209) had SNPs at the 2000 bp region upstream of the start codon, and there was no difference in the nucleotide sequences of other*
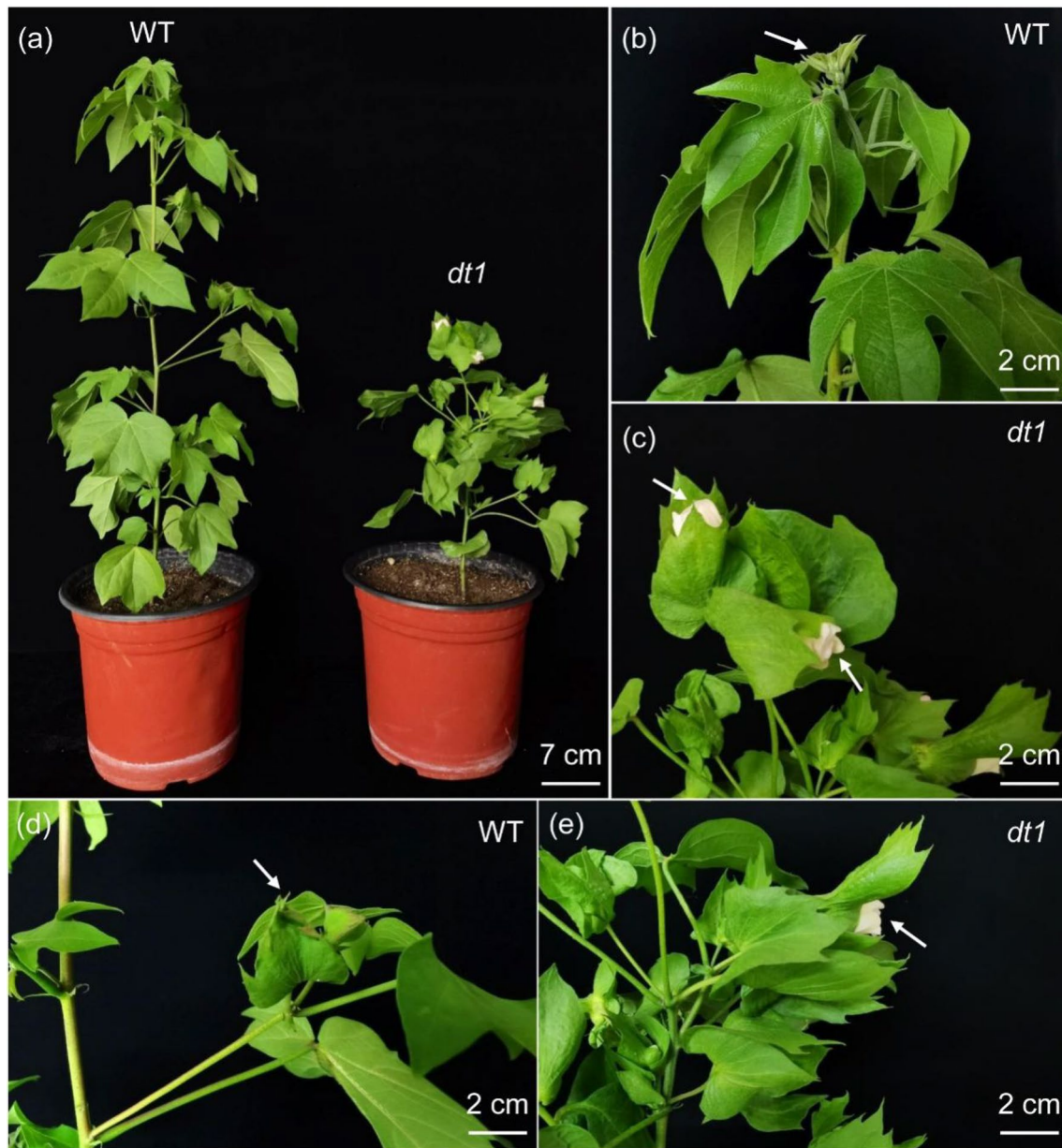
Fig. 1 The phenotype of determinate growth and indeterminate growth in *dt1* and wild type Shixiya 1. **a** The plant architecture of the *dt1* mutant and the wild type Shixiya 1 (Scale bar = 7 cm) at the flower bud stage. **b–c** The destiny of the shoot apical meristem (SAM) in the *dt1* mutant and the wild type Shixiya 1. The white arrow indicates that the SAM became terminal flowers in the *dt1* mutant (**c**) compared with the young leaf formed in the wild type Shixiya 1 (**b**) (Scale bar = 2 cm). **d–e** The fruit branch of the *dt1* mutant and the wild type Shixiya 1. The white arrow indicates that the axillary buds of the lateral branches became flower buds in the *dt1* mutant (**e**) compared with the young leaf formed in the wild type Shixiya 1 (**d**) (Scale bar = 2 cm)

genes between the two parents (Fig. S1). Furthermore, semi-quantitative expression analysis indicated that only *Ga07G1189*, *Ga07G1195* and *Ga07G1207* displayed significant changes in transcription between Shixiya 1 and *dt1*, while other 9 genes didn't show clear alteration in transcription during the floral differentiation (Fig. S2). In addition, we further analyzed the three candidate genes. *Ga07G1189* was annotated as "*terminal flower 1a* [*Gossypium hirsutum*]", which was related to the determinate growth of many plants including *G. hirsutum* and *G. barbadense* (Chen et al. 2018; Kotoda et al. 2006; Njogu et al. 2020; Si et al. 2018). Moreover, the putative ORF from genomic DNA and RNA indicated that the single SNP represents an RNA 5′ splice site mutation from G to A (at the 201st position of the first exon) in the *dt1* mutant compared with the wild type Shixiya 1,
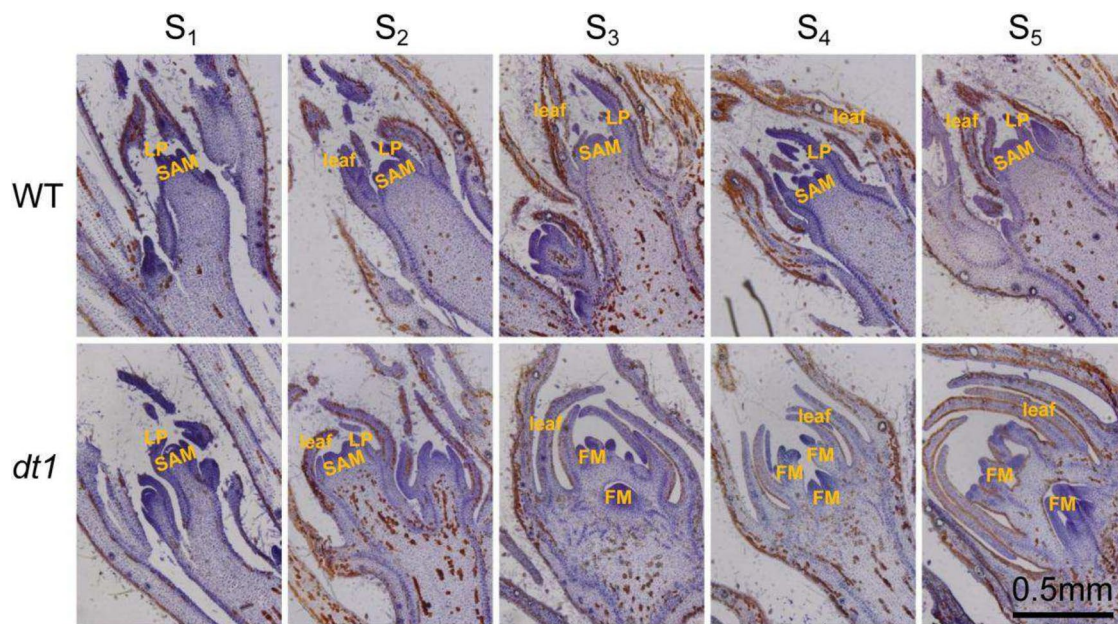
Fig. 2 The long section analysis of the terminal buds. Microscopic observation of the terminal buds slices from one to five true leaf stages (from S1 to S5) in the *dt1* mutant and the wild type Shixiya 1. LP stands for leaf primordium, SAM stands for shoot apical meristem and FM stands for floral meristem. Scale bar = 0.5 mm

and results in a 93-bp deletion from 108 to 200 bp in the coding sequence (CDS), as well as a 31 amino (VYN-GHEFFPSAVTNKPKVEVHGGDMRSFFTL) deletion of *Ga07G1189* (*GaTFL1*) first exon in the *dt1* (Fig. 3c and Fig. S3). Regarding other two genes (*Ga07G1195* and *Ga07G1207*), no change in the mRNA sequence or amino acids sequence were identified except the transcription level. Therefore, we identified *Ga07G1189* as the potential candidate gene of *dt1*. Further, semi-quantitative expression analysis revealed that the *GaTFL1* transcription was significantly higher in the wild-type Shixiya 1 than that in the *dt1* mutant (Fig. S4).

The GU–AG rule is conserved in RNA splicing (Wang and Burge 2008). Through analysis of the transcripts and the alternative splicing in *Ga07G1189* between the WT and the *dt1* mutant, a novel splice site G/GT (boundary sequence of the first exon and intron) before the original splice site was identified to produce a shorter mature RNA and fewer amino acids, which was also confirmed by the sequencing of RT-PCR and genome PCR of *Ga07G1189* (Fig. S3), the primers used to amplify coding regions and full genomic regions of *Ga07G1189* gene were listed in Table S1. We also analyzed splicing profiles in *TFL1* of other plants, which confirmed the same and conserved 5′ splice site GU (or GT) in different *TFL1s*, and revealed that site G/GT was a novel splicing site of G/GT in *TFL1* loci (Fig. 3d). This finding suggested that other GT sites in genomic DNA which have not been recognized as splice sites previously might become the potential RNA splicing sites when plants encounter some specific stimuli to help plant change the function and survive.

Silencing of *GaTFL1* results in terminal flowers similar to those in *dt1* phenotype plants

To further test the function of *GaTFL1*, a 302 bp fragments including the first exon of *GaTFL1* was cloned and inserted into pTRV2 for VIGS. After 2 months postinfiltration, the TRV: *GaTFL1* consistently displayed terminal flowers, resulting in a determinate architecture compared to that in leaves infiltrated with a blank TRV: 00 vector (Fig. 4a), which was similar to the *dt1* phenotype plants, qRT-PCR analysis revealed that the expression of each respective *GaTFL1* in root, stem, leaf and flower bud tissues was much lower in *GaTFL1*-silenced plants compared with that in blank vector control TRV: *00* plants (Fig. 4b), indicating that *GaTFL1* may be the key gene for the indeterminate growth phenotype associated with the *dt1* locus.

Analysis of differentially expressed genes between Shixiya 1 and *dt1*

To gain insight into the network and mechanism underlying the determinate growth development in *dt1*, RNA-Seq was performed with the terminal buds of Shixiya 1 and *dt1* at

Fig. 3 Fine mapping and cloning of *determinate growth 1*. **a** QTL analysis of the determinate growth phenotype in an F_2 segregating population, the determinate growth locus was mapped on chromosome A07 from 7.31 Mb to 24.57 Mb. The red arrow indicates the only window with a ΔSNP value exceeding the 99% significance threshold confidence interval across the whole genome. The ΔSNP index (SNP index of the determinate growth bulk population subtracted from that of the indeterminate growth bulk population) and its 99% confidence interval are shown as black curves and red dotted lines (ΔSNP index > 0.5), respectively. **b** Genetic mapping of the determinate growth locus in a population with 150 F_2 recessive individual plants by KASP. The number of recombinants was shown below the blue line. **c** The alternative 5′ splice site from GG to AG mutation in the first exon of *Ga07G1189* resulted in a 31 amino acids (VYNGHEFFPSAVTNKPKVEVHGGDMRSFFTL) deletion in the putative protein sequence. **d** The G/GT splice site in *TFL1* loci of other plants. In the gray dot box, the original G/GT splice site of *GaTFL1* is marked in red and other G/GT sites are marked in orange
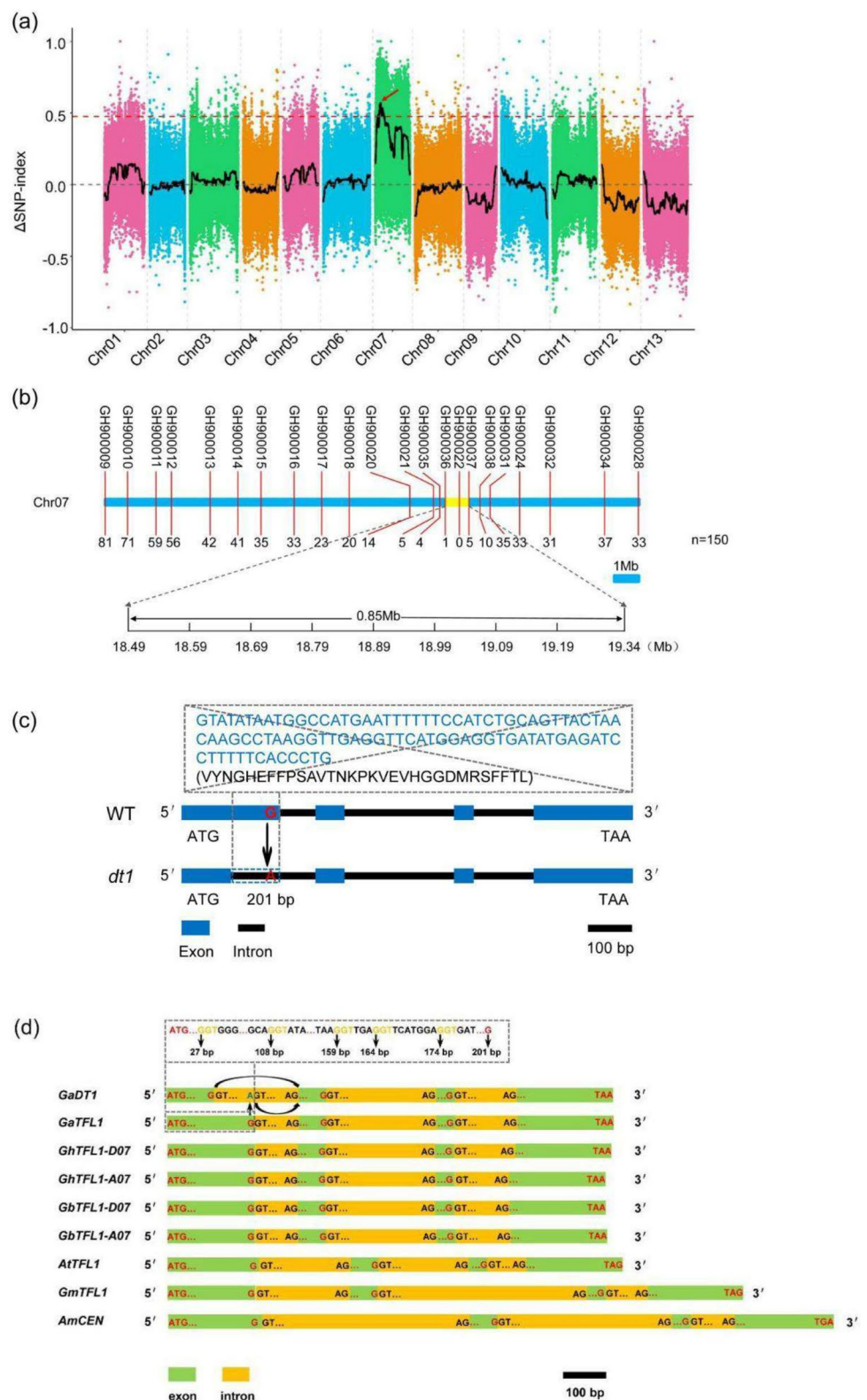
different stages T_1 (seedling stage, three true leaves), T_2 (the early stage of flower bud formation, no visible flower buds), and T_3 (flower budding stage, with visible flower buds) to analyze the DEGs in the different stages with an adjusted *P*-value < 0.05 and an absolute value of fold change ≥ 2.0. In total, 7133 gene transcripts were identified, of which 471 were expressed at three stages, 5003 were stage-specific and 1659 were expressed at two stages. Strikingly, more

Fig. 4 Silencing of *GaTFL1* results in terminal flower plants similar to *dt1* phenotype. **a** The phenotype of *Gossypium arboreum* line DQJ after silencing endogenous *GaTFL1* and blank vector infiltration plants. The red arrow indicates that the SAM became terminal flower in TRV: *GaTFL1* plant compared with the young leaf formed in blank vector control TRV: *00* plant, and the white arrow indicates that the axillary buds of the lateral branches became flower buds in TRV: *GaTFL1* plant compared with the young leaf formed in blank vector control TRV: *00* plant. **b** The level of *GaTEL1* transcript in different tissues of *GaTFL1*-silenced (TRV: *GaTFL1*) plants and the negative control (TRV: *00*). Two-tailed Student *t*-test was used for paired comparison of the *GaTFL1* gene in TRV: *GaTFL1* and TRV: *00* different tissues, respectively (**$P < 0.01$ or *$P < 0.05$)
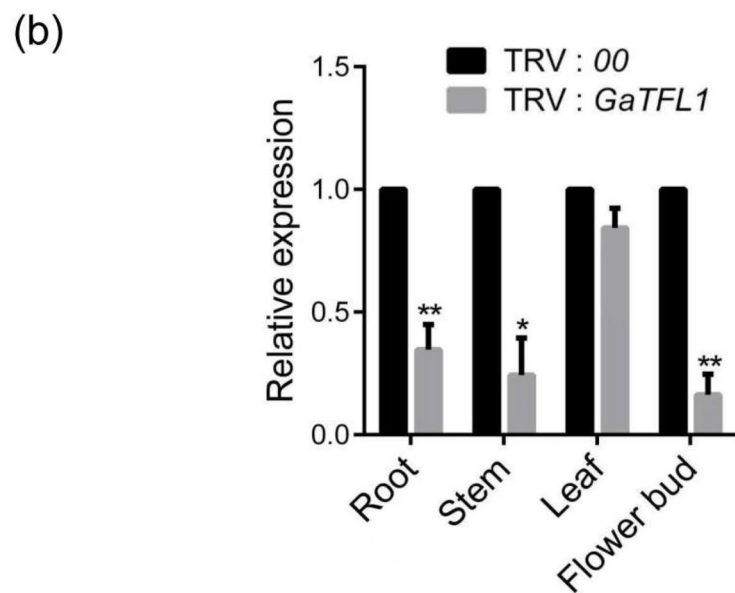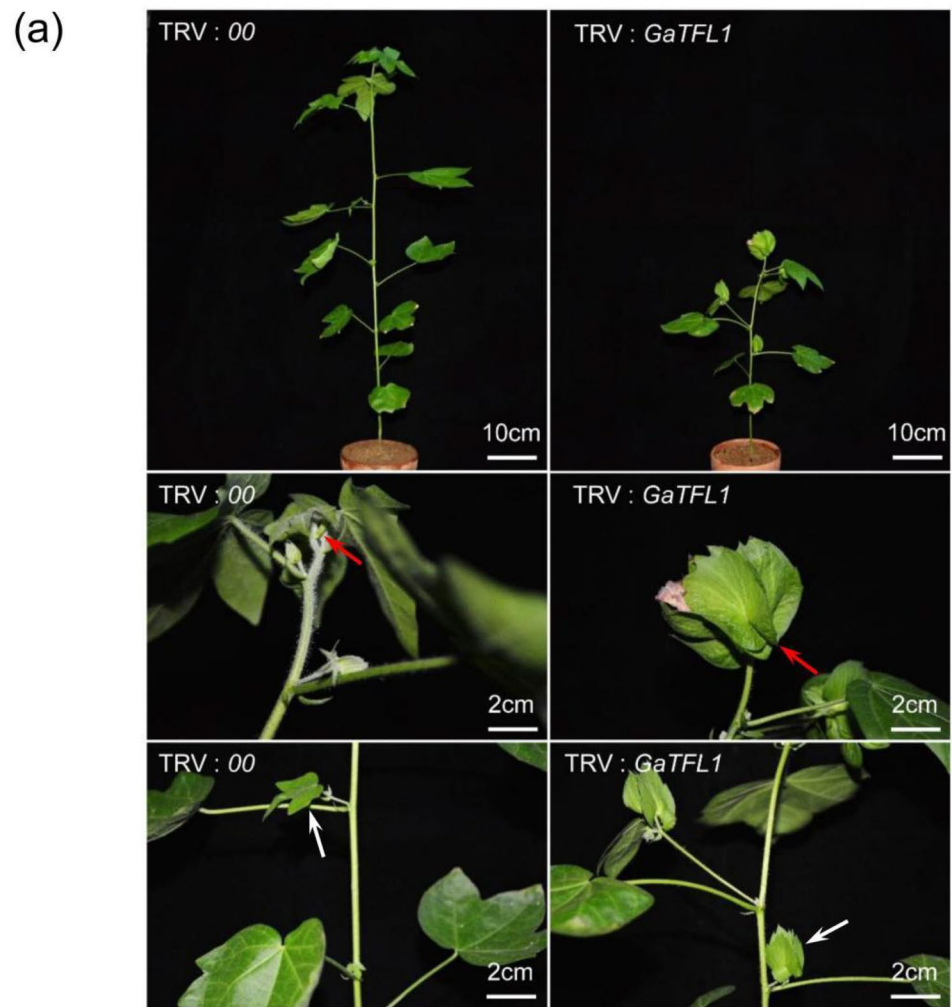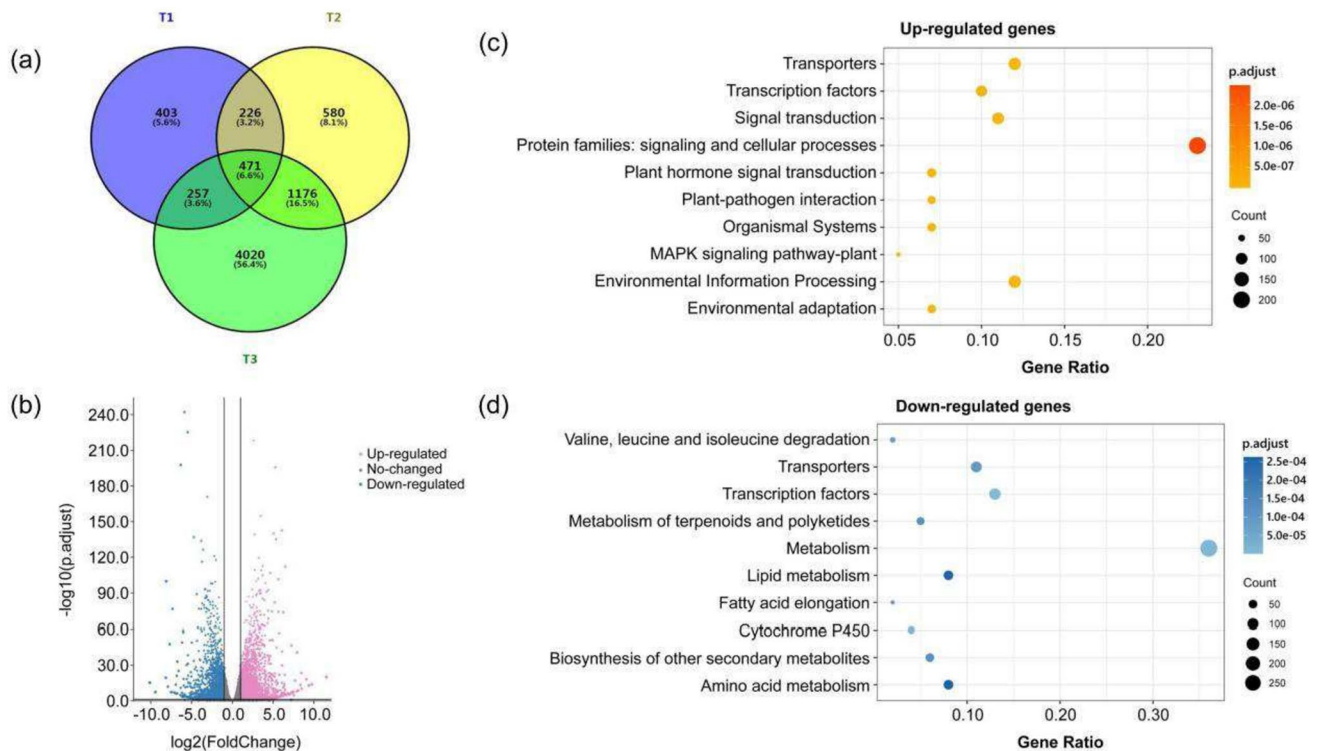
Fig. 5 Transcriptomic comparison of the *dt1* mutant versus Shixiya 1. **a** Venn diagram showing the overlaps between the different stages of the *dt1* mutant and Shixiya 1. The number above each stage designation is the total transcripts detected in that stage(s). **b** Volcano plot of differentially expressed genes (DEGs) between the terminal bud of the *dt1* mutant and Shixiya 1 at T_3 stage (flower budding stage, with visible flower buds). **c** The top 10 KEGG enriched pathways of up-regulated genes. **d** The top 10 KEGG enriched pathways of down-regulated genes. The top 10 KEGG enriched pathways are selected by p. adjust value sorting. Count, the bubble size, represents the number of enriched genes. GeneRatio represents the ratio of the number of DEGs corresponding to the pathway to the number of DEGs corresponding to the pathway database

stage-specific DEGs (4020) were identified in the T_3 stage than that in the T_1 (403) and T_2 (580) stages (Fig. 5a), which was consistent with the phenotype at stage T3 when the *dt1* mutant formed the top flower resulting in the determinate growth phenotype. This indicates that many specific genes are involved in the regulation of the determinate growth in the T3 stage of *dt1*. A total of 5924 DEGs were identified in the T_3 stage, including 3239 up-regulated and 2685 down-regulated genes (Fig. 5b and Table S4).

To reveal the causal genes and the underpinning resulting in the determinate growth of *dt1*, we performed KEGG analysis for the DEGs at the T_3 stage. The KEGG enrichment analysis showed that both up-regulated and down-regulated genes related to transporters (e.g., MATE efflux family, Sugar transporter, ABC transporter) and transcription factors were enriched significantly (Fig. 5c, d). Seven MATE efflux family genes were up-regulated (Table S5), of which MATE1 and MATE2 genes are associated with the pleiotropic phenotypes of plants, such as leaf length, flowering time (Tiwari et al. 2014). Besides, 14 MATE efflux family proteins were down-regulated

(Table S5), including one DTX1 protein and three ALF5 members, which positively regulated lateral root formation and increase root sensitivity to various compounds (Diener et al. 2001), and three TRANSPARENT TESTA 12-like proteins were involved in flavonoid transport (Marinova et al. 2007). Nine up-regulated and five down-regulated ABC transporters encoding genes were identified (Table S5), of which *ABCB19*, *ABCB1*, *ABCB21*, and *ABCB15* show redundant function and positively regulate auxin transport and plant height (Dudler and Hertig 1992). In addition, ten down-regulated genes involved in the sugar transport family, including five SWEET proteins and two SUC2-like proteins (Table S5), of which SWEET proteins may be involved in *Arabidopsis* inflorescence development (Chen et al. 2010, 2012; Yuan and Wang 2013). These results, to some extent, revealed the reasons for the different differentiation ability of terminal buds and the formation of terminal flowers in the *dt1* mutant and provided clues for the mechanisms of TFL1 in indeterminate growth regulation.

Protein structure analysis reveals the functional divergence of TFL1 mutations in different *Nulliplex-branch* cottons

The previous research has identified several TFL1 mutants in different *Nulliplex-branch* (*nb*) mutants such as *Ghnb-1*, *Ghnb-2*, *Ghnb-3*, *Ghnb-4*, *Gbnb-1* (Chen et al. 2018; Si et al. 2018), which all display indeterminate growth of main stem and short fruit branches that terminate in a cluster of two or more flowers (Fig. 6a–c). The *Gadt1* displays determinate growth of main stem with a terminal flower and causes one or more clustered flowers with elongated pedicels to be attached directly to the main stem

Fig. 6 The protein structure and plant architecture analysis of the different types of *TFL1* alleles. **a** The 3D protein structure of TFL1 and plant architecture of indeterminate growth cotton. The amino acids of the first exon is marked in gray, of which the 31 amino acids deletion of *dt1* in the first exon is marked in light blue. **b** The 3D protein structure of Ghnb-1 to Ghnb-4 and plant architecture of *Ghnb* phenotype. The amino acids of the first exon is marked in gray, and the mutation of D73N amino acid is marked in purple. **c** The 3D protein structure of Gbnb-1 and plant architecture of *Gbnb* phenotype. The amino acids of the first exon is marked in gray, and the mutation of P113S amino acid is marked in bule. **d** The 3D protein structure of Gadt1 and plant architecture of *Gadt1* phenotype. Amino (N) and carboxy (C) termini are labeled. White arrows in (**a**), (**b**) and (**c**) represent the missing β-sheets in (**d**). Green triangles represent monopodial SAMs, blue triangles represent sympodial SAMs, black arrows represent vegetative branches, and red circles represent bolls
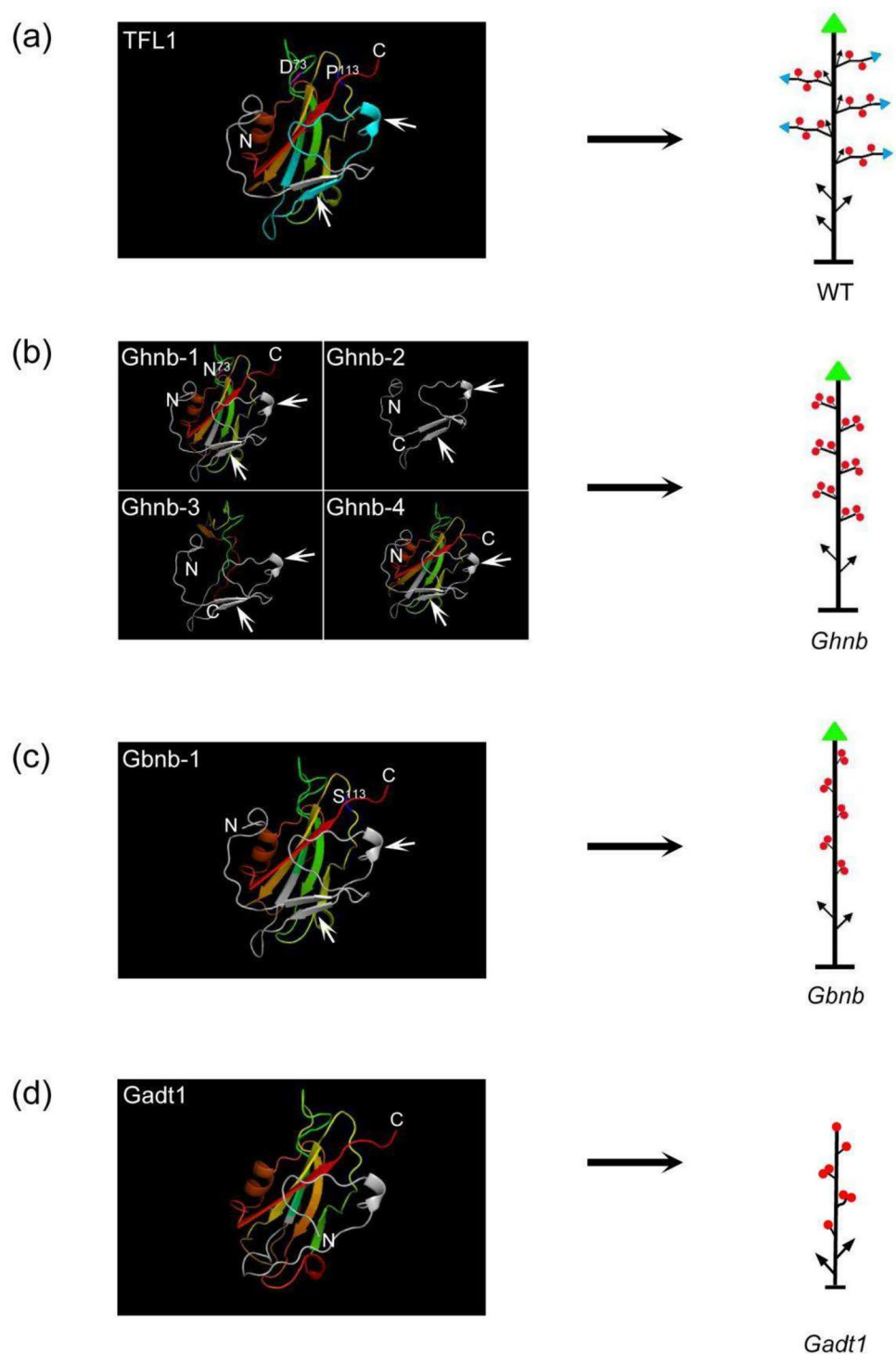
(Fig. 6d), whose determinate growth habit of main stem differed significantly from the other *nb* lines (Fig. 6a–c). The difference in plant architecture phenotypes between *Gadt1* and other *nb* mutants indicates the potential protein functional divergence of different TFL1 mutations. For *Ghnb* lines, four mutations within the CDS region were detected, namely, a single nucleotide mutation from G to A at position 217 in exon 2, causing a non-synonymous amino acid change, D73N (designated as Ghnb-1), a single T deletion at position 194 in exon 1, a two nucleotide deletion at positions 254–255 in exon 2, and a single T deletion at position 491 in exon 4 (designated as Ghnb-2 to Ghnb-4, respectively). For *Gbnb* line, a single nucleotide mutation from C to T at position 337 in exon 4, caused a non-synonymous amino acid change, P113S (designated as Gbnb-1) (Chen et al. 2018). For Gadt1, a single nucleotide mutation from G to A at position 201 in exon 1, changed the 5′ splice site and deleted 31 amino acid (Fig. 3c). To explore the protein tertiary structure differences among them, we used Phyre2 to predict the 3D structure of the mutational TFL1 in the different *nb* lines, and found that there was no significant difference in the corresponding protein structures of the first exon of Ghnb-1, Ghnb-2, Ghnb-3, Ghnb-4 and Gbnb-1 compared with the WT, harboring the unabridged β-sheets and pocket (Fig. 6a–c). However, the novel mutant Gadt1 displayed a novel variation of 3D structure for the truncated protein, showing two β-sheets missing (Fig. 6a,d), which may damage the intact pocket and the key function of TFL1 protein to result in the change in both main stem and lateral branches.

Discussion

The domestication of crops prefers more determinate architectures with compact growth habits and synchronous flowering. Therefore, comprehending the underlying mechanism leading to the difference between indeterminate and determinate growth can benefit crop improvement. Generally, indeterminate plants produce inflorescence on flanks, while determinate plants generate a flower or inflorescence at the top. Many factors have been identified involved in the inflorescence and plant architecture regulation, among which the FT-TFL1 model has been identified as the key factor with antagonistic functions in inflorescence and plant architecture controlling (Teo et al. 2014; Wickland and Hanzawa 2015).

A single nucleotide mutation alters the splicing pattern in the *TFL1* locus

Cotton species displays naturally indeterminate growth. Under favorable conditions, both of the main stem and the lateral branches remain indeterminate growth (Fig. 6a).

However, several determinate growth lines such as Caozao-3 (*nb*-type upland cotton), Xinhai-18, (*nb*-type Pima cotton) and a modern ELS cultivars (extra-long-staple cotton (AD)2, *G. barbadense* L.) have been recognized in tetraploid lines, and the determinate growth trait can be stably inherited. Further studies also explored the detailed nucleotide in the above *nb* mutants (Chen et al. 2018; Si et al. 2018). In the present study, we also identified a similar *determinate growth 1* (*dt1*) mutant in diploid line Shixiya 1 (*G. arboreum*) with the EMS mutagenesis approach. The gene cloning revealed that the determinate growth phenotype in all the above lines is controlled by the various mutations in the same *TFL1* locus, supporting the vital role of TFL1 in plant architecture regulation. So, we analyzed the mutation sites in the *TFL1* locus of *G. arboreum* and uncovered that a novel single nucleotide mutation from G to A at the 201st position changed the splicing site of the first exon/intron and produced a shorter exon, which generated a truncated protein with loss of function. Moreover, *Gadt1* also showed some different plant architecture changes compared with other *nb* cottons. The prediction and analysis of 3D structure of the mutational TFL1 in the different *nb* lines revealed a novel variation of 3D structure for the truncated protein of Gadt1 (Fig. 6d), suggesting that different domains or amino acids of TFL1 may have distinct function to contribute to the plant architecture regulation. Further, we also analyzed the splicing sites in other *TFL1* genome sequences from *Arabidopsis thaliana*, *Glycine max*, and *Antirrhinum majus*. These findings indicated that G/GT but not A/GT is a recognizable site of RNA splicing in the plant *TFL1* loci, which provided potential targets for the *TFL1* gene editing by CRISPR-Cas9 technology as well as some clues for the gene alternative splicing sites study in the plant. However, several other G/GT sites were also found around the original splice G/GT (201st bp) of *TFL1* (Fig. 3d), why they are not recognized in *dt1* by the spliceosome is still unclear. Understanding the detailed mechanisms of interaction between spliceosome and *TFL1* pre-mRNA with the Hi-C technology, specific site mutation technology et al. would contribute to explore the underpinning for alternative splicing in *GaDT1*. These results indicated the diversity and specificity of alternative splicing mechanisms and spliceosomes in cells.

The mechanisms of TFL1 in the indeterminate growth of the plant

Based on previous research, it was proposed that the balance of determinate and indeterminate growth in all plants is controlled by the balance of the activities of the FT and TFL1 homolog gene products (Lifschitz et al. 2014, 2006; Pnueli et al. 1998; Shalit et al. 2009). The mutation of TFL1 alters the inflorescence architecture and results in the determinate

growth in different plants, and contributes to the crop yield, mechanical harvest, and human domestication such as cotton, tomato, and soybean (Chen et al. 2018; Pnueli et al. 1998; Tian et al. 2010). While the underlying mechanism that TFL1 regulates inflorescence and plant architecture is still ambiguous. In general, TFL1 and FT compete for the interaction with FD to involve the floral organ and inflorescence formation as mobile factors (Benlloch et al. 2007; Hanano and Goto 2011; Liljegren et al. 1999; Ratcliffe et al. 1999). Interestingly, both of them also bind TFL1 and FT are distinct through only a little part of nonconservative amino acid changes, supporting their common binding ability with FD and lipid di 18:1-PC (Chen et al. 2018), although they display antagonistic roles (Ho and Weigel 2014; Ahn et al. 2006). A single amino acid substitution can convert FT into TFL1 and vice versa (Ho and Weigel 2014; Ahn et al. 2006; Hanzawa et al. 2005; Pin et al. 2010). So, minor amino acids change might influence the TFL1 function obviously, which may be realized through the delicate adjustment on the function domain or the 3D structure of protein. The results from this study further provide valuable clues to elucidate the complex and fine interaction between FT and TFL1 in the inflorescence regulation. In both FT and TFL1, a large central β-sheet and a smaller β-sheet comprise the important pocket motif, which are resulted from the first exon (Ahn et al. 2006). Further structural analysis of TFL1 suggests that its pocket is able to accommodate phosphoryl groups but not phospholipid, suggesting the potential signaling mediation by TFL1 via their association with phosphorylated proteins (Pnueli et al. 2001). The previous interaction and activity inhibition between a mouse PEBP and the kinase Raf1 also supported the possibility (Yeung et al. 1999). Therefore, the GaDT1 seems disturb the upstream signaling transduction in the formation of SAM and axillary meristem simultaneously to affect the plant architecture. Through some technologies such as Nuclear Magnetic Resonance (NMR) and Immunoprecipitation-Mass Spectrometry (IP-MS), the specific interactors with the pocket or β-sheets in the first exon could be identified, which would be very beneficial to reveal the TFL1 function mechanism and explain the difference between different TFL1 mutants.

In a word, the exhaustive study for every amino acid or nucleotide, and the unidentified regions of protein would be necessary to explore the function of TFL1/FT, as well as the underlying mechanism for the competition between FT and TFL1 for FD. In cucumber, CsTFL1 competes with CsFT for interaction with a homolog of the miRNA biogenesis gene, CsNOT2a. Then, the complex interacts with CsFDP (Wen et al. 2019). These indicated that TFL1 may be involved in different molecular and physiological pathways. Even so, the detailed downstream pathway of TFL1 is unclear. Here, we performed an RNA-Seq with the terminal SAM tissues in *dt1* mutant and WT to propose a model (Fig. 7). After the DEGs analysis, some transporters responsible for the auxin, sugar, and flavonoids are enriched downstream of TFL1 in the determinate growth regulation (Table S5). Massive literature reported that auxin and sugar play important roles in SAM to regulate inflorescences and plant architecture establishment (Vernoux et al. 2010; Xing et al. 2015; Yoon et al. 2021; Zhu and Wagner 2020), indicating that TFL1 associated complex or functional models are involved in the transport and translocation of key metabolites or phytohormones for the SAM tissue development. The previous direct interaction between TFL1 and NOT2a or lipid (Chen et al. 2018; Wen et al. 2019) suggested that TFL1 might regulate the transporters' expression and function through epigenetic modification (i.e., miRNA mediated gene regulation) or cell membrane permeability mediation, bridging the link between TFL1 and the transport of key materials such as auxin, sucrose and flavonoids to regulate plant architecture and inflorescence (Fig. 7). In previous studies, the FT-TFL1 model, auxin, and sugar are known as the important factors in inflorescence and plant architecture, but the correlation among them is always unclear. The results of this study demonstrated that TFL1 may function upstream of the auxin and sugar pathways by mediating their transport to coordinate the vegetative and reproductive development from the SAM (Fig. 7). Some genetic research or biochemistry experiments with immunoprecipitation of TFL1 antibody would be helpful to elucidate the detailed relationship between TFL1 and transporters.

Conclusion

The *dt1* mutant in *G. arboreum* was identified through EMS mutagenesis, which displayed determinate growth in both of the SAM and axillary buds with a terminal flower. The map-based cloning of the *DT1* locus showed a single nucleotide mutation from G to A at the 201st position changed the 5′ RNA splice site and deleted 31 amino acid in the first exon of *GaTFL1*, which is a novel mutation site different from the Ghnb-1, Ghnb-2, Ghnb-3, Ghnb-4 and Gbnb-1. Comparative transcriptomic RNA-Seq analysis indicated that GaTFL1 may function upstream of auxin, sugar, and

Fig. 7 The hypothesis model of functional mechanism of TFL1 in plant architecture regulation. TFL1 associated complex are involved in the transport and translocation of sugar, key metabolites (e.g., flavonoids, toxin) or phytohormones (e.g., auxin) for the SAM tissue development. In these processes, TFL1 interacts with NOT2a or lipid di 18:1-PC to regulate the expression and function of genes encoding transporters responsible for auxin, sugar, flavonoids and toxin through epigenetic modification pathway or direct structure modification. With this mechanism, TFL1 function upstream of the auxin, sugar, flavonoids and toxin transport pathways to coordinate the vegetative and reproductive development and plant architecture. (Red circles around TFL1 represent lipid di 18:1-PC; Green triangles represent monopodial SAMs, blue triangles represent sympodial SAMs, black arrows represent vegetative branches, and red circles represent bolls)
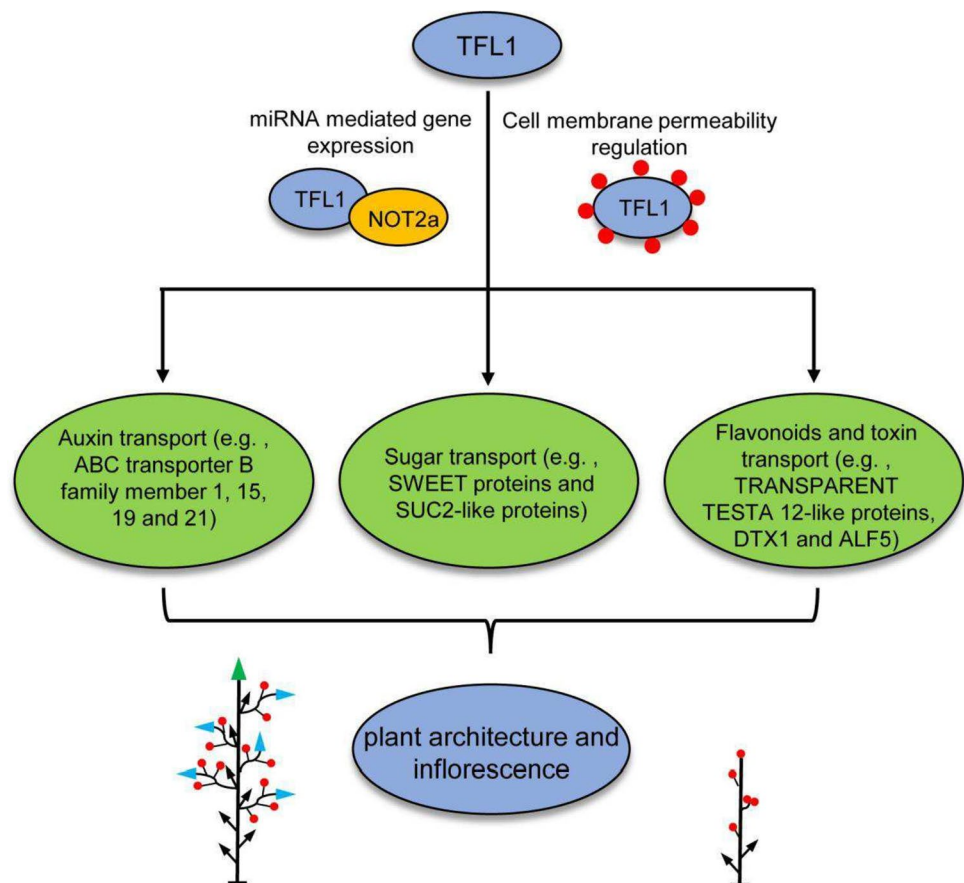
flavonoids. Taken together, our results contribute to explore the diversity and specificity of alternative splicing mechanisms and spliceosomes in cells and provide novel clues for the TFL1 mechanism in plant development regulation and research strategies for plant architecture improvement.

Author contribution statement JL and ZW planned and designed the research; PM, WQ, WH, ZW, WD, and HZ performed experiments; PM analyzed data; JL, PM and ZW wrote the manuscript, and all authors read and approved the final manuscript.

Data availability All the data sets generated during the current study are available in the NCBI Sequence Read Archive (SRA) under project number PRJNA989558 for BSA-seq and PRJNA989394 for RNA-seq.

Declarations

Conflict of interest The authors declare that they have no conflict of interest.

Ethical approval The authors declare that the experiments comply with the current laws of China.

References

Ahn JH, Miller D, Winter VJ, Banfield MJ, Lee JH, Yoo SY, Henz SR, Brady RL, Weigel D (2006) A divergent external loop confers antagonistic activity on floral regulators FT and TFL1. EMBO J 25:605–614

Akhtar KP, Haidar S, Khan MKR, Ahmad M, Sarwar N, Murtaza MA, Aslam M (2010) Evaluation of Gossypium species for resistance to cotton leaf curl Burewala virus. Annals of Applied Biology 157:135–147

Amasino RM, Michaels SD (2010) The timing of flowering. Plant Physiol 154:516–520

Baumann K, Venail J, Berbel A, Domenech MJ, Money T, Conti L, Hanzawa Y, Madueno F, Bradley D (2015) Changing the spatial pattern of TFL1 expression reveals its key role in the shoot meristem in controlling *Arabidopsis* flowering architecture. J Exp Bot 66:4769–4780

Benlloch R, Berbel A, Serrano-Mislata A, Madueno F (2007) Floral initiation and inflorescence architecture: a comparative view. Ann Bot-London 100:659–676

Boss PK, Bastow RM, Mylne JS, Dean C (2004) Multiple pathways in the decision to flower: enabling, promoting, and resetting. Plant Cell 16:S18–S31

Bradley D, Carpenter R, Copsey L, Vincent C, Rothstein S, Coen E (1996) Control of inflorescence architecture in Antirrhinum. Nature 379:791–797

Bradley D, Ratcliffe O, Vincent C, Carpenter R, Coen E (1997) Inflorescence commitment and architecture in *Arabidopsis*. Science 275:80–83

Chen LQ, Hou BH, Lalonde S, Takanaga H, Hartung ML, Qu XQ, Guo WJ, Kim JG, Underwood W, Chaudhuri B, Chernak D, Antony G, White FF, Somerville SC, Mudgett MB, Formmer WB (2010) Sugar transporters for intercellular exchange and nutrition of pathogens. Nature 468(7323):527–532

Chen LQ, Qu XQ, Hou BH, Sosso D, Osorio S, Fernie AR, Formmer WB (2012) Sucrose efflux mediated by SWEET proteins as a key step for phloem transport. Science 335(6065):207–211

Chen W, Yao JB, Li Y, Zhao LJ, Liu J, Guo Y, Wang JY, Yuan L, Liu ZY, Lu YJ, Zhang YS (2018) Nulliplex-branch, a TERMINAL FLOWER 1 ortholog, controls plant growth habit in cotton. Theor Appl Genet 132(1):97–112

Diener AC, Gaxiola RA, Fink GR (2001) *Arabidopsis* ALF5, a multi-drug efflux transporter gene family member, confers resistance to toxins. Plant Cell 13(7):1625–1638

Dudler R, Hertig C (1992) Structure of an mdr-like gene from *Arabidopsis thaliana*. J Biol Chem 267(9):5882–5888

Eberwein R, Nickrent DL, Weber A (2009) Development and morphology of flowers and inflorescences in Balanophora papuana and B. elongata (Balanophoraceae). Am J Bot 96:1055–1067

Gong Q, Yang ZE, Wang XQ, Butt HI, Chen EY, He SP, Zhang CJ, Zhang XY, Li FG (2017) Salicylic acid-related cotton (*Gossypium arboreum*) ribosomal protein GaRPL18 contributes to resistance to *Verticillium dahlia*. BMC Plant Biol 17:59

Gong Q, Yang ZE, Chen EY, Sun GF, He SP, Butt HI, Zhang CJ, Zhang XY, Yang ZR, Du XM, Li FG (2018) A Phi-class glutathione S-transferase gene for Verticillium wilt resistance in *Gossypium arboreum* identified in a genome-wide association study. Plant Cell Physiol 59(2):275–289

Hanano S, Goto K (2011) *Arabidopsis* TERMINAL FLOWER1 is involved in the regulation of flowering time and inflorescence development through transcriptional repression. Plant Cell 23:3172–3184

Hanzawa Y, Money T, Bradley D (2005) A single amino acid converts a repressor to an activator of flowering. Proc Natl Acad Sci U S A 102:7748–7753

Ho WW, Weigel D (2014) Structural features determining flower-promoting activity of *Arabidopsis* FLOWERING LOCUS T. Plant Cell 26:552–564

Jack T (2004) Molecular and genetic mechanisms of floral control. Plant Cell 16:1–17

Jia YP, Li KX, Liu HD, Zan LX, Du DZ (2019) Characterization of the BnA10.tfl1 gene controls determinate inflorescence trait in Brassica napus L. Agronomy 9(11):722

Kotoda N, Iwanami H, Takahashi S, Abe K (2006) Antisense expression of MdTFL1, a TFL1-like gene, reduces the juvenile phase in apple. J Am Soc Hortic Sci 131:74–81

Langmead B, Salzberg S (2012) Fast gapped-read alignment with Bowtie 2. Nat Methods 9(4):357–359

Li H, Handsaker B, Wysoker A, Fennell T, Ruan J, Homer N, Marth G, Abecasis G, Durbin R, Proc G (2009) The sequence alignment/map format and SAM tools. Bioinformatics 25:2078–2079

Li Z, Li L, Zhou KH, Zhang YH, Han X, Ding YP, Ge XY, Qin WQ, Wang P, Li FG, Ma ZY, Yang ZE (2019) GhWRKY6 acts as a negative regulator in both transgenic *Arabidopsis* and cotton during drought and salt stress. Front Genet 10:392

Lifschitz E, Eviatar T, Rozman A, Shalit A, Goldshmidt A, Amsellem Z, Alvarez JP, Eshed Y (2006) The tomato FT ortholog triggers systemic signals that regulate growth and flowering and substitute for diverse environmental stimuli. Proc Natl Acad Sci U S A 103:6398–6403

Lifschitz E, Ayre BG, Eshed Y (2014) Florigen and anti-florigen—a systemic mechanism for coordinating growth and termination in flowering plants. Front Plant Sci 5:465

Liljegren SJ, Gustafson-Brown C, Pinyopich A, Ditta GS, Yanofsky MF (1999) Interactions among APETALA1, LEAFY, and TERMINAL FLOWER1 specify meristem fate. Plant Cell 11:1007–1018

Livak KJ, Schmittgen TD (2001) Analysis of relative gene expression data using real-time quantitative PCR and the $2 - \Delta\Delta CT$ method. Methods 25:402–408

Marinova K, Pourcel L, Weder B, Schwaez M, Barron D, Routaboul JM, Debeaujon I, Klein M (2007) The *Arabidopsis* MATE transporter TT12 acts as a vacuolar flavonoid/H+-antiporter active in proanthocyanidin-accumulating cells of the seed coat. Plant Cell 19:2023–2038

McGarry RC, Prewitt SF, Culpepper S, Eshed Y, Lifschitz E, Ayre BG (2016) Monopodial and sympodial branching architecture in cotton is differentially regulated by the *Gossypium hirsutum* SINGLE FLOWER TRUSS and SELF-PRUNING orthologs. New Phytol 212:244–258

Mehetre SS, Aher AR, Gawande VL, Patil VR, Mokate AS (2003) Induced polyploidy in Gossypium: a tool to overcome interspecific incompatibility of cultivated tetraploid and diploid cottons. Curr Sci India 84:1510–1512

Nibouche S, Brevault T, Klassou C, Dessauw D, Hau B (2008) Assessment of the resistance of cotton germplasm (Gossypium spp.) to aphids (Homoptera, Aphididae) and leafhoppers (Homoptera, Cicadellidae, Typhlocybinae): methodology and genetic variability. Plant Breed 127:376–382

Njogu MK, Yang F, Li J, Wang X, Ogweno JO, Chen J (2020) A novel mutation in TFL1 homolog sustaining determinate growth in cucumber (Cucumis sativus L.). Theor Appl Genet 133:3323–3332

Pin PA, Benlloch R, Bonnet D, Weich EW, Kraft T, Gielen JJL, Nilsson O (2010) An antagonistic pair of FT homologs mediates the control of flowering time in sugar beet. Science 330:1397–1400

Pnueli L, Carmel-Goren L, Hareven D, Gutfinger T, Alvarez J, Ganal M, Zamir D, Lifschitz E (1998) The SELF-PRUNING gene of tomato regulates vegetative to reproductive switching of sympodial meristems and is the ortholog of CEN and TFL1. Development 125:1979–1989

Pnueli L, Gutfnger T, Hareven D, Ben-Naim O, Ron N, Adir N, Lifschitz E (2001) Tomato SP-interacting proteins define a conserved signaling system that regulates shoot architecture and flowering. Plant Cell 13:2687–2702

Ratcliffe OJ, Bradley DJ, Coen ES (1999) Separation of shoot and floral identity in *Arabidopsis*. Development 126:1109–1120

Sethi K, Siwach P, Verma SK (2015) Assessing genetic diversity among six populations of *Gossypium arboreum* L. using microsatellites markers. Physiol Mol Biol Plants 21(4):531–539

Shalit A, Rozman A, Goldshmidt A, Alvarez JP, Bowman JL, Eshed Y, Lifschitz E (2009) The flowering hormone florigen functions as a general systemic regulator of growth and termination. Proc Natl Acad Sci U S A 106:8392–8397

Shannon S, Meeks-Wagner DR (1991) A mutation in the *Arabidopsis* TFL1 gene affects inflorescence meristem development. Plant Cell 3:877–892

Si ZF, Liu H, Zhu JK, Chen JD, Wang Q, Fang L, Gao FK, Tian Y, Chen YL, Chang LJ, Liu BL, Han ZG, Zhou BL, Hu Y, Huang XZ, Zhang TZ (2018) Mutation of SELF-PRUNING homologs in cotton promotes short-branching plant architecture. J Exp Bot 69(10):2543–2553

Tahir MS, Khan NUI, Sajid-Ur-Rehman (2011) Development of an interspecific hybrid (triploid) by crossing *Gossypium hirsutum* and *G. arboreum*. Cytologia 76(2):193–199

Teo ZWN, Song SY, Wang YQ, Liu J, Yu H (2014) New insights into the regulation of inflorescence architecture. Trends Plant Sci 19:158–165

Tian Z, Wang X, Lee R, Li Y, Specht JE, Nelson RL, McClean PE, Qiu L, Ma J (2010) Artificial selection for determinate growth habit in soybean. Proc Natl Acad Sci U S A 107:8563–8568

Tiwari M, Sharma D, Singh M (2014) Expression of OsMATE1 and OsMATE2 alters development, stress responses and pathogen susceptibility in *Arabidopsis*. Sci Rep 4:1–12

Trapnell C, Williams B, Pertea G, Mortazavi A, Kwan G, van Baren M, Salzberg S, Wold B, Pachter L (2010) Transcript assembly and quantification by RNA-Seq reveals unannotated transcripts and isoform switching during cell differentiation. Nat Biotechnol 28:511–515

Vernoux T, Besnard F, Traas J (2010) Auxin at the shoot apical meristem. Csh Perspect Biol 2(4):a001487

Wang Z, Burge CB (2008) Splicing regulation: from a parts list of regulatory elements to an integrated splicing code. RNA 14:802–813

Wen CL, Zhao WS, Liu WL, Yang LM, Wang YH, Liu XW, Xu Y, Ren HZ, Guo YD, Li C, Li JG, Weng YQ, Zhang XL (2019) CsTFL1 inhibits determinate growth and terminal flower formation through interaction with CsNOT2a in cucumber. Development 146(14):dev180166

Wheeler TA, Gannaway JR, Keating K (1999) Identification of resistance to Thielaviopsis basicola in diploid cotton. Plant Dis 83:831–833

Wickland DP, Hanzawa Y (2015) The FLOWERING LOCUS T/TERMINAL FLOWER 1 gene family: functional evolution and molecular mechanisms. Mol Plant 8:983–997

Wu J, Liu YA, Tang L, Zhang FL, Chen F (2011) A study on structural features in early flower development of Jatropha curcas L. and the classification of its inflorescences. Afr J Agr Res 6(2):275–284

Xing LB, Zhang D, Li YM, Shen YW, Zhao CP, Ma JJ, An N, Han MY (2015) Transcription profiles reveal sugar and hormone signaling pathways mediating flower induction in apple (Malus domestica Borkh.). Plant Cell Physiol 56:2052–2068

Yeung K, Seitz T, Li S, Janosch P, McFerran B, Kaiser C, Fee F, Katsanakis KD, Rose DW, Mischak H, Sedivy JM, Kolch W (1999) Suppression of Raf-1 kinase activity and MAP kinase signalling by RKIP. Nature 401:173–177

Yoon J, Cho LH, Tun W, Jeon JS, An G (2021) Sucrose signaling in higher plants. Plant Sci 302:110703

Yuan M, Wang SP (2013) Rice MtN3/saliva/SWEET family genes and their homologs in cellular organisms. Mol Plant 6(3):665–674

Zhu Y, Wagner D (2020) Plant inflorescence architecture: the formation, activity, and fate of axillary meristems. Csh Perspect Biol 12(1):a034652